small NANO MICRO

Inkjet-Printed Multicolor Arrays of Highly Luminescent Nanocrystal-Based Nanocomposites

Joo Yeon Kim, Chiara Ingrosso, Vahid Fakhfouri, Marinella Striccoli, Angela Agostiano, M. Lucia Curri, and Jurgen Brugger*

Inkjet technology is a compelling method for the flexible and cost-effective printing of functional inks. We show that nanocomposite solutions based on polystyrene and differently sized core/shell-type nanocrystals (NCs) formed by a CdSe core coated with a shell of ZnS (CdSe@ZnS) in a single solvent, chloroform, can be reliably dispensed into luminescent, multicolor pixel arrays. This study demonstrates the relevance of parameters like polymer concentration and nozzle diameter, highlighting how the optimal conditions to print NCs embedded in 5 wt% polystyrene nanocomposite are given by a 70-μm-diameter nozzle. The obtained structures show that the bright size-dependent emission of the NCs in the nanocomposite is retained in the printed pixels.

Keywords:
- colloidal nanocrystals
- inkjet printing
- multicolor arrays
- nanocomposites
- polystyrene

1. Introduction

The ability to pattern functional materials is of paramount importance in the fabrication of integrated micro-/nanosystems such as miniaturized sensors or actuators, as well as photonic, electronic, microfluidic, bioanalytical, and biomedical devices. Conventional vacuum depositions and photolithographic patterning methods involve heat treatment and full substrate surface exposure to photoresist and thus do not allow the processing of fragile and sensitive substrates. In addition, such techniques are not the most suitable for the fabrication of complex structures, requiring fabrication of multiscale and multilevel features on nonplanar or even curved surfaces. Currently, such limitations can be overcome by means of the most recent direct-writing techniques,[1] such as local dispensing[2] and contact-free direct inkjet printing.[3] Such emerging patterning methods, across multiple length scales, rely on the direct, local, and accurate deposition of minute quantities of solutions, dispersions, and melts from an inkjet print-head or nozzle on substrates ranging from silicon, glass, quartz, and polymer to ''paper-like'' flexible materials. Microscale patterns can be simply designed and fabricated in relatively arbitrary 2D and (quasi-)3D shapes, without requiring any vacuum process, spin-coating, removal step, or expensive lithographic masks and equipment. Moreover, direct writing techniques enable a convenient ''add-on'' placement of microscale features, even onto prepatterned substrates. In addition, a low material consumption is granted, thus avoiding wasting, which represents a crucial issue when high value and expensive materials are used. In addition, high-throughput capability and high cost-effectiveness can be achieved when automated equipment, like commercial inkjet printers, are used. Directly written microstructures have recently been integrated into innovative transistor architectures by using polymers,[4] or used as catalysts for carbon nanotube (CNT) growth,[5] in light-emitting devices (LEDs),[6] solar cells,[7] and biosensors, and in cell printing for tissue engineering.[8] Material libraries and multicomponent systems such as 2D multicolor polymer LEDs have even been fabricated by means of combinatorial material printing strategies by using multi-nozzle or, alternatively, sequential printing approaches.[9]

Recent advances in material science have further extended the potential of inkjet printing technology, by designing and

[*] Dr. M. L. Curri, Dr. C. Ingrosso, Dr. M. Striccoli, Prof. A. Agostiano
CNR-IPCF sez. Bari, c/o Dip. di Chimica, Università di Bari
via Orabona 4-I, 70126 Bari (Italy)
E-mail: lucia.curri@ba.ipcf.cnr.it
Dr. J. Y. Kim, Dr. V. Fakhfouri, Prof. J. Brugger
Microsystems Laboratory
Ecole Polytechnique Fédérale de Lausanne (EPFL)
CH-1015 Lausanne (Switzerland)
Dr. C. Ingrosso, Prof. A. Agostiano
Dip. di Chimica, Università di Bari
via Orabona 4-I, 70126 Bari (Italy)

Supporting Information is available on the WWW under http://www.small-journal.com or from the author.

DOI: 10.1002/smll.200801315

synthesizing colloidal nanoparticles (NPs) and nanocrystals (NCs) characterized by unique size- and shape-dependent properties, and by an exceptionally convenient processing capability. Thus NCs can be considered excellent candidates for developing original functional inks and are formidable candidates for innovative inkjet deposition routes and a variety of applications. NPs and NCs can be synthesized by colloidal chemistry approaches[10] to properly tune electronic, magnetic, or photocatalytic properties by simply tailoring size and geometry. In addition, this synthetic method provides NCs with an ideal interface with their external environment since the layer of organic molecules coordinated at the NC surface allows them to be treated as macromolecules. This characteristic enables their dispersion and positioning in any chemical environment and consequently their integration in 2D or 3D assembled structures and composites. In particular, resists and thermoplastic nanocomposites incorporating NCs have been recently achieved, allowing the fabrication of a new generation of purposefully designed microcomponents based on NPs with tailored properties and defined functions.[11]

In recent years, different papers have shown that the accurate study of inkjet printing conditions in an appropriate experimental setup allows the fabrication of inks based on complex functional NP composites in which the outstanding properties of the nano-objects are transferred to the final microstructures. As an example, metal NPs have been deposited and their size dependent decrease in melting temperature has allowed the fabrication of microelectronic components at low temperature, such as metal lines and microcontacts onto polymeric substrates,[12] as well as the fabrication of organic field effect transistors (OFETs).[13] Moreover, functionalized CdTe NC–poly(vinyl alcohol) (PVA) composites have been dispensed in microstructures in which the size tunable emission of NCs has been exploited for the generation of combinatorial libraries.[14]

Exploitation of the great potential of II–VI semiconductor NC-based inks is currently hindered by the limited choice of a carrier medium, which should simultaneously be convenient for homogeneously disperse NCs and suited for inkjet printing. For this class of materials, the common solvent should preserve the optical characteristics of both the NCs and the polymeric matrix, as well as their prompt processability by providing uniform nanocomposites. At the same time, the carrier must preserve suitable properties, namely viscosity, surface tension, boiling point, and volumetric homogeneity in the final material, which are key parameters for reliable droplet formation in drop-on-demand dispensing.

Here nanocomposite inks based on polystyrene (PS) and highly luminescent NCs formed by a CdSe core coated with a shell of ZnS (CdSe@ZnS) have been prepared and deposited as single- and multicolor microscale arrays. PS with a molecular weight of 5200 g mol^{-1} was selected for its attractive properties of flexibility, good processing capability, and high optical transparency, which render it a good candidate for containers, packaging, and light diffusion elements.[15] Green-, orange-, and red-emitting organic soluble CdSe@ZnS NCs, in size ranging from 2.7 to 4.6 nm and coated by trioctylphosphine oxide (TOPO) surfactant molecules, were synthesized. According to the procedure reported in the experimental section, their size-dependent emission characteristics were conveyed to the PS-based inks.

Nanocomposite preparation was carried out by exploiting the characteristic solubility of these colloidal NCs in an apolar solvent and by selecting a single-component common medium that is able to safely disperse presynthesized organic-capped NCs in the host polymer matrix. A common solvent was selected in order to preserve the distinctive properties of the functional NCs (i.e., to prevent aggregation and quenching phenomena) and to remain simultaneously compatible with the typical inkjet printing conditions. A low boiling point (61.5 °C) solvent, $CHCl_3$, was used to locally dispense nanocomposite solutions based on differently sized CdSe@ZnS NCs and different PS concentrations with a stable and reproducible droplet generation.

2. Results and Discussion

In Figure 1 the steady state absorption and photoluminescence (PL) emission spectra of the differently sized TOPO capped CdSe@ZnS NCs in $CHCl_3$ and in PS-based nanocomposites are reported. The spectroscopic characteristic absorption spectra of the colloidal CdSe@ZnS NCs show a main excitation peak attributed to the first optically allowed transition, blue-shifted with respect to the bulk CdSe. Average NC diameters are typically obtained from the wavelength position of the absorption edge.[16] The CdSe@ZnS NC PL emission spectra are characterized by a strong and narrow band edge emission as expected from the low size dispersion of the NCs in solution. The relative PL quantum yields of

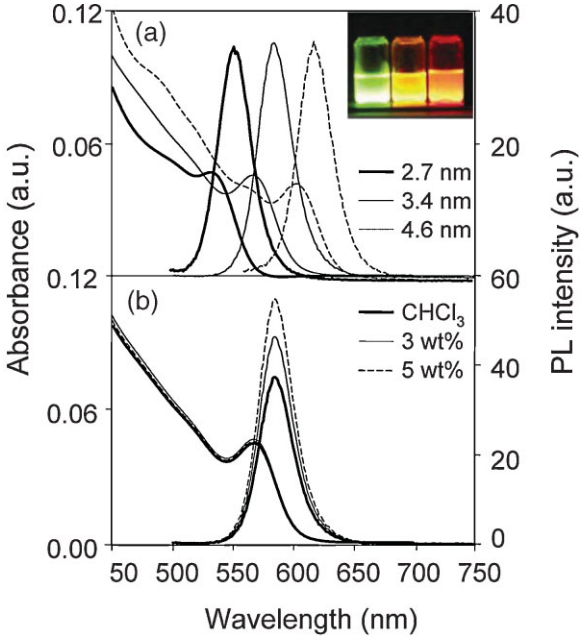

Figure 1. Steady state UV–Vis absorption and PL emission spectra of a) the 2.7-, 3.4-, and 4.6-nm diameter CdSe@ZnS NCs in $CHCl_3$ at the excitation wavelength of 400 nm (inset: photograph of CdSe@ZnS NCs in $CHCl_3$ under an UV lamp), and b) 3×10^{-7} M CdSe@ZnS NCs (3.4-nm-diameter) in $CHCl_3$ and CdSe@ZnS NCs embedded in 3 and 5 wt% PS nanocomposites in $CHCl_3$ at the excitation wavelength of 500 nm.

NANO MICRO small

2.7-, 3.4-, and 4.6-nm-diameter CdSe@ZnS NCs are 54%, 34%, and 50%, respectively. The steady state absorption and PL emission spectra of the nanocomposites formed of CdSe@ZnS NCs and 3 and 5 wt% of PS in $CHCl_3$ are compared with those of the bare NCs in the same solvent. The characteristic NC optical properties upon their incorporation in PS are retained without any shift of the absorption spectra towards longer absorption wavelength, thus indicating that no NC coalesced aggregates or ripening phenomena have occurred. Remarkably, the NC PL emission intensity increases once incorporated in PS, and this PL enhancement appears proportional to the weight percentage of PS in the composite. The relative PL quantum yield value of the 3.4-nm CdSe@ZnS NCs increases up to 43.5% and to 51% in the nanocomposites containing 3 and 5 wt% of PS, respectively, and the same behavior has been observed for NCs of different sizes. This enhancement can be reasonably accounted for by a variation of the dielectric confinement effect in PS with respect to $CHCl_3$. Indeed, a decrease of the dielectric constant and refractive index values takes place passing from the $CHCl_3$ to the PS solutions.[17] This hypothesis is confirmed by the observed increase of the effect at higher PS content in the composite.

Inkjet printing was performed by using a piezo-actuated inkjet printer from Microdrop Technologies (Scheme 1). The nozzle was actuated in squeeze mode. Two nozzles having diameters of 70 and 100 μm, respectively, were used to print pixels of single- or multidrops. The generation of drops was observed with a stroboscopic system when tuning the generating signal amplitude and pulse length of the piezo-actuator. The pressure in the inkjet nozzle was controlled to optimize the liquid flow, the wetting of the nozzle, and the ejection properties. The substrate was positioned relatively to the printing nozzle with a motorized high-precision *x*-*y*-*θ* stage (Scheme 1). For the multiprinting process, three different nozzles having same diameter were mounted side-by-side above the moving substrate stage. Each nozzle was optimized individually to match the appropriate parameters to generate stable drops. The inkjet printing performances of $CHCl_3$ solutions of PS with concentrations of the polymer ranging from 1 to 5 wt% were investigated to determine the suitable polymer solution for inkjet printing. To deposit the prepared inks, both continuous and drop-on-demand (DOD) inkjet modes and different diameter nozzles were used in order to determine the most suitable printing conditions by using the setup reported in Scheme 1 and described in the experimental section.

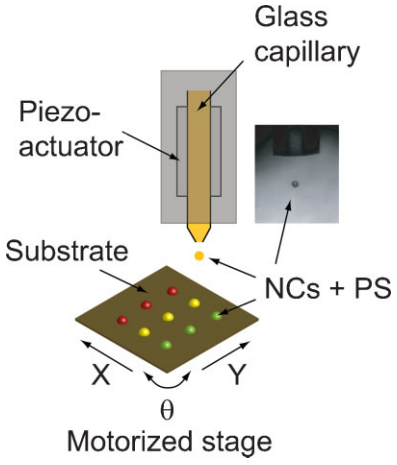

Scheme 1. Schematic representation of the inkjet setup. A glass capillary is actuated in squeeze mode by a piezoactuator. A pressure wave is generated that leads to the generation of microdrops. A computer-controlled motorized *x*-*y*-*θ* stage precisely positions the substrate under the printing head. NC-doped PS solutions are deposited in continuous and DOD modes. The inkjet printing performances of PS solutions in toluene and $CHCl_3$ with concentrations ranging from 1 to 5 wt% were investigated to determine the suitable polymer solution for inkjet printing. The inset is the stroboscopic image of the drops, generated by inkjet printing. This picture shows a Newtonian fluid behavior.

The following phenomena can affect negatively a stable and reliable micropatterning: i) clogging of the nozzle, ii) formation of satellite drops and filaments, and iii) alteration of the shape of the surface structures by accumulation of the ink at the feature edges[3] due to the so-called ''coffee-staining effect''. These effects are conditioned by the combined characteristics of ink, nozzle, and surface. For instance, nozzle clogging typically occurs when the ink used is composed of suspensions or when the fluid characteristics, such as viscosity, change during the deposition. Satellites and filaments form when the fluid has a high viscosity and a very low surface tension, or when the liquid is heterogeneous on a spatial scale on the order of the sizes of the fluid jet diameter. In addition, this occurrence can be a consequence of rapid and inhomogeneous solvent evaporation.[3] To limit such phenomena, the main approaches adopted so far relay on i) filtering the fluid or operating in a particle-controlled environment, ii) using a single solvent-based ink formed of water and alcoholic solutions or high boiling point solvents (i.e., anisole, dioxane, xylene, ethylacetate, acetophenone, etc.), iii) dispensing two solvent-based ink solutions, in which one solvent has a high boiling point,[3,9] iv) substrate heating,[14] and v) depositing inside spatially confined hydrophobic barriers, that is, barriers made by plasma surface treatment. Isopropyl acetate/acetophenone solutions have been used as solvents in the inkjet printing of Ru- and Ir-based complexes in premade patterned features,[9] and thioglycolic acid and 3-mercaptopropionic acid have been employed as additives in composite inks of CdTe NCs and PVA to limit the coffee-staining ring effect.[14] n-Tetradecane has been selected as a solvent to dispense 33–70 wt% AgNP solutions filtered with a 0.20 μm filter, and alpha-terpinol has been used to dispense 10 wt% AuNP solutions.[12,13]

In this work, several parameters were found to affect the stability, reproducibility, and final dimension of the printed microstructures, namely i) number of drops, ii) size of NCs, and iii) concentration of PS. Indeed, the inkjet printing conditions were systematically adjusted based on stroboscopic observation while monitoring in real-time the dynamics of drop generation. Pixels of 25 or 50 droplets were deposited by using a dedicated computer-controlled protocol that carefully counts the number of droplets per pixel by synchronizing the inkjet nozzles with the *x*- and *y*-stage parameters. The deposited microstructures were morphologically characterized by means of optical and fluorescence microscopy, scanning electron microscopy (SEM), optical profilometry,

and atomic force microscopy (AFM). These investigations show that self-standing pixels were dispensed in reproducible concave disk-like microstructures with an almost negligible coffee-staining effect. These promising results attest that original NC-based inks, formed of a single low boiling point solvent, in our case $CHCl_3$, provide reliable inkjet processing even onto glass, which is known to cause spreading of organic solvents without any control over environmental conditions (i.e., temperature, pressure, and humidity), filtering, pretreatment of the substrate, or occurrence of nozzle clogging.

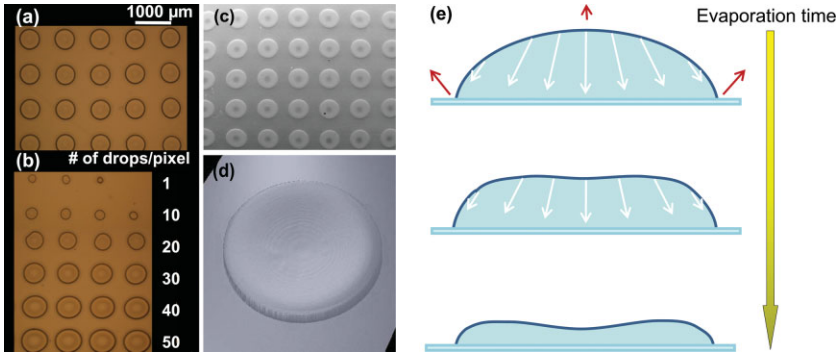

Figure 2. a) Optical microscopic images of inkjet-printed 25-drop-pixels. b) Different numbers of drops per lines. c) SEM and d) optical profiler 3D images of 25-drop-pixels inkjet-printed using 3.4-nm-diameter NCs embedded 5 wt% PS nanocomposite in $CHCl_3$. e) Schematic cross sectional view of the droplet surface during solvent evaporation.

The inkjet printing behavior of PS solutions in $CHCl_3$ was tested in continuous and DOD modes with nozzles with different sizes (70- and 100-μm diameters, respectively). Continuous mode here means that the droplets are ejected at high frequency (2–3 kHz) without interruption, providing the possibility for stroboscopic investigation and stable drop generation by minimizing solvent evaporation. On the contrary, DOD mode signifies that the ejection of individual droplets can be controlled at any desired time and position. The latter configuration obviously offers higher flexibility but is more demanding in terms of inkjet printing parameters. Our study was mainly concentrated towards DOD mode. To this end, the stability and reproducibility of drop formation and ejection under different experimental conditions were monitored and the results are summarized in Table 1.

The 100-μm-diameter nozzle generated unstable drops with $CHCl_3$, probably due to the high evaporation rate of the solvent, which induces a rapid local changing in ink properties and consequently hinders efficient nozzle control. Hence the 70-μm-diameter nozzle was preferred in DOD mode. More stable and reproducible drops were obtained at higher PS concentration due to the optimized solvent evaporation rate at the nozzle to prevent the incrustation of PS nanocomposites. The molecular weight and concentration of the polymeric composite was found to play an important role in the formation of filaments during the inkjet printing process, on which the stability of the generated drops depends.[18]

Table 1. Summary of the stability and reproducibility of inkjet printing with various concentrations of PS in $CHCl_3$ using two nozzle diameters (70 and 100 μm).

		Nozzle			
		100 μm		70 μm	
	Print mode	Continuous mode	DOD mode	Continuous mode	DOD mode
PS-concentration	1 wt%	[a]	[a]	[c]	[b]
	2 wt%	[a]	[a]	[c]	[b]
	3 wt%	[a]	[a]	[c]	[c]
	4 wt%	[a]	[a]	[c]	[c]
	5 wt%	[a]	[a]	[c]	[d]

[a] No stable drop generated. [b] Stable drops generated but not reproducible. [c] Reproducible stable drops generated. [d] Reproducible stable drops generated, but the generation is very sensitive to the evaporation of the solvent and the pressure.

One important parameter for polymer inkjet printing is the viscoelastic property when passing through the nozzle where the shear rate can be as high as 1×10^5 s^{-1}.[18a] In fact, polymeric inks with high molecular weights or high polymer concentrations show a non-Newtonian behavior characterized by the fluid viscosity dependence on the applied strain rate, resulting in a noticeable presence of long filaments and satellite drops. [18a] We investigated the inkjet-ability of PS concentration ranging from 1 to 5 wt% at a molecular weight of 5200 g mol^{-1} and no pronounced long filament and satellite formation were observed. In view of optimizing the polymer concentration, we therefore selected the two PS concentration values of 3 and 5 wt% for further investigation. In Figure 2 optical microscope images of inkjet-printed pixels (25 drops per pixel) of 3.4-nm CdSe@ZnS NCs in 5 wt% PS, show a regular shape without any satellite with a pixel diameter around 600 μm, which is indicative of stable inkjet printing conditions. In particular, it was noticed that when pixels are formed of less than 20 drops, the surface geometry is less reproducible (Figure 2b), a setback known as the "first-drop-issue".[19] Furthermore, by analyzing the pixel morphology, no pronounced coffee-staining effect was observed (Figure 2c), in spite of the fact that the pixels were printed by using a single-solvent ink. Optical microscopy and SEM allow the analysis of the 3D topography of the inkjet-printed pixels (Figure 2d), indicating only a slight concavity in the central region of the droplets, as inferred by the slight change in shading in both the optical and SEM images. Figure 2e displays an illustration of droplet profile evolution as function of time during solvent evaporation. A non-uniform speed of solvent evaporation, which decreases in passing from the center of the droplet to the edges (red arrows), could be ascribed to a solute redistribution and substrate–solute interactions (white arrows).[20]

The inkjet printing of CdSe@ZnS NC nanocomposites was performed by systematically varying the experimental parameters (Table 2). The droplet diameter is shown to slightly enlarge when the polymer concentration is increased. Indeed, when the polymer concentration increases a higher voltage and pulse length are required to obtain a stable ejection,

NANO MICRO small

Table 2. Summary of inkjet printing parameters of CdSe@ZnS NC-embedded PS nanocomposites in $CHCl_3$.

		3 wt%			5 wt%		
		Sizes of the NCs [nm]					
Inkjet parameters		2.7	3.4	4.6	2.7	3.4	4.6
Voltage [V]			112			135	
Pulse length [μs]			51			124	
Frequency [Hz]			2097			3111	
Pixel Diameter [μm]	25[a]		≈400–480			≈550–620	
	50[b]		≈590–610			≈700–800	

[a] 25 drops per pixel. [b] 50 drops per pixel.

resulting in a larger droplet volume to be ejected. The optimized settings were then used to print single- and multicolor arrays formed of 25 and 50 drop pixels of CdSe@ZnS NC nanocomposites based on 5 wt% PS. The fluorescence optical microscope images of single-color arrays are shown in Figure 3.

Once the single-nozzle printing conditions were optimized, experiments were extended towards parallel printing by using multiple nozzles, each one loaded with a different ink, in view of truly multi-material flexible inkjet printing. To this end, one print-head per color was used and the printing parameters were adjusted once for each. A vertically installed microscope allowed the determination of the impact position of the droplets on the substrate. The alignment was done by defining the droplet impact position with respect to a reference point and subsequently correcting the *x*-*y* position in order to precisely locate the target under the nozzle. In the multi-nozzle system, the alignment steps were carried out for one print-head and, based on the distance between the drop impact-point of each head with respect to the first head, an offset value per head was determined and used for aligned multicolor printing with higher accuracy. In addition, when appropriately programmed, this multi-nozzle inkjet printing system can be operated both time and cost effectively for a large variety of pattern configurations in view of large-scale applications (up to several tens of centimeters). Using this system, three-color arrays were successfully printed by using a three-nozzle system, one nozzle per color, with high position and alignment accuracy between the three colors coming from the three different nozzles (Figure 3). Here, NCs embedded in 3 wt% PS nanocomposites in $CHCl_3$ (1×10^{-5} M) were used and the droplets were generated by using an appropriate voltage, pulse length, and frequency, depending on the different nozzle/material system (Table 2). During the inkjet printing process, the substrate positioned under the multi-nozzle system was then moved in computer controlled *x*,*y*-directions to the next position.

The morphology of the inkjet-printed CdSe@ZnS NC nanocomposite pixels was then investigated in order to evaluate the surface quality of the microstructures. In Figure 4 the 2D views of the topographic AFM images of the pixels formed of bare PS and ink nanocomposites containing differently sized NCs are compared. These results show that pure PS-based pixels present a rather smooth surface (<1 nm root mean square (rms) roughness), whereas a significant change (1–3 nm rms roughness) is observed for the

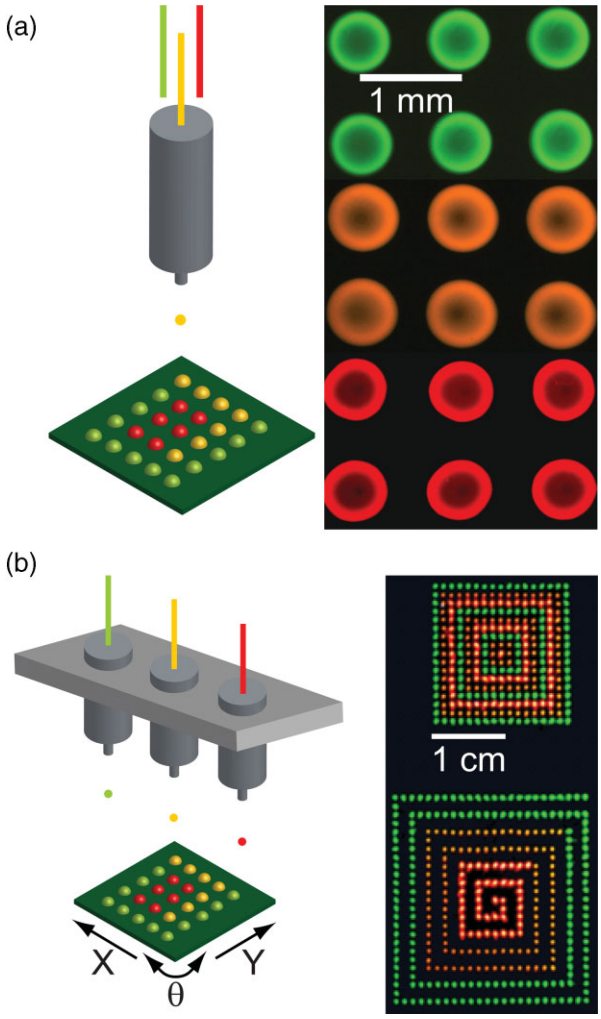

Figure 3. a) Single-nozzle system. Optical microscopy images of part of a 9×9 single-color array. Fluorescent nanocomposite arrays individually inkjet printed on a glass substrate with differently sized CdSe@ZnS NC-embedded 5 wt% PS nanocomposites with a ≈550–620 μm range of pixel size. b) Multi-nozzle system. Fluorescent photograph of inkjet-printed multicolor pixels with differently sized CdSe@ZnS NC-embedded 3 wt% PS nanocomposites excited by an UV lamp at 366 nm. CdSe@ZnS NCs sized 2.7, 3.4, and 4.6 nm correspond to green, orange, and red emissions, respectively, and each pixel has 25 drops with 1 mm pitches.

nanocomposites. In the latter case, the topography is mainly characterized by irregular nanometer-sized features protruding from the surface. The height of such structures enhances with increasing NC diameter, but almost no change is observed with an increase in the number of inkjet-printed droplets. The dimensions of such features significantly exceed the CdSe@ZnS NC size, being likely due to NC aggregation or inhomogeneous assembling induced by interdigitation of the ligand alkyl chains at the NC surfaces.[11] Figure 4d shows the change of the pixel rms roughness with the NC size compared to the bare PS pixels. Indeed, irrespective of the number of the dispensed droplets, this value increases significantly with respect to the bare PS microstructures. In particular, the pixels based on nanocomposites containing larger NCs (4.6-nm

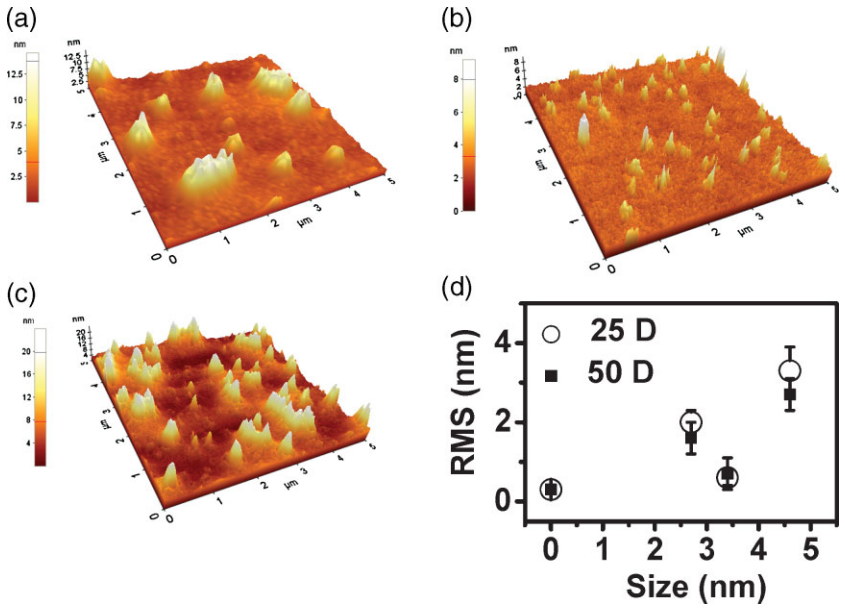

Figure 4. a–c) 2D AFM images (5 μm × 5 μm) of inkjet-printed 25-drop-pixels with 5 wt% PS nanocomposites with 2.7-, 3.4-, and 4.6-nm-diameter CdSe@ZnS NCs. d) rms roughness value of inkjet-printed pixels with CdSe@ZnS NCs embedded in 5 wt% PS nanocomposites. The value corresponding to 0 nm refers to the bare PS pixel.

diameter) show a higher rms roughness, while only a small increase is observed for those containing 3.4-nm-diameter NCs, which is even smaller than the value recorded for the pixels containing the smallest NCs. A trend is also reflected in the roughness values measured on nanocomposite films spin-coated onto glass. This behavior could probably be ascribed to the effect of the NC size and curvature, which modifies the extent to which the capping ligand surface coverage forms aggregates, whose dimensions are NC-size-dependent.[21]

3. Conclusions

The reported results highlight the effectiveness of inkjet printing in fabricating microstructures formed of functional nanocomposites. The unconventional deposition technique reveals great potential for generating reproducible pixels with careful control over the shape once the suitable deposition parameters are defined. The excellent dispersibility of the highly luminescent NCs in an apolar solvent is a result crucial for the preparation of highly processable inks with no need for multiple-solvent mixtures or post-preparative processing. Luminescent polymeric microstructure arrays were obtained by using both a single- and a multi-nozzle approach. The results allow the manufacture of highly luminescent, non-bleachable, and conveniently structured processable nanocomposites by inkjet printing, which are useful for mono- and multicolor polymer displays and colored wall papers. In addition, the same approach can be extended to functionalize a variety of polymers not only with luminescent NCs, but also with magnetic or conducting NCs in order to fabricate polymer-based micro- and nanoelectronic components drop-by-drop, where the combination of the approach with conductive polymers would allow the realization of novel displays based on polymeric light-emitting diodes (PLEDs). Finally, inkjet printing is technique that allows the local and precise addition of material without any further processing steps, and that saves time and precious material, thus resulting in an exceptionally versatile surface printing technique for costly functional polymers.

4. Experimental Section

Materials: All chemicals were of the highest purity available and used as received without further purification. CdO (powder, 99.5%), Se (powder, 99.99%), TOPO (99% and technical grade), tetrabutylphosphinic acid (TBPA, 97%), hexadecylamine (HDA, 90%), tributylphosphine (TBP, 99%), diethylzinc ($C_4H_{10}Zn$, 1.0 M solution in heptane), hexamethyldisilathiane ($C_6H_{18}Si_2S$, synthesis grade), nonanoic acid ($C_9H_{18}O_2$, 96%), $CHCl_3$ (>99.8%), and toluene (99%) were purchased from Aldrich. PS (MW 5200 g mol^{-1}) and hexane (99%) were purchased from Alfa Aesar and Fluka, respectively.

Synthesis of CdSe@ZnS NCs: CdSe NCs were synthesized by injecting a TBP solution of Se in a hot mixture of HDA, TOPO, TBPA, and CdO. Typically this reaction leads to the formation of NCs having diameters of 2.7, 3.4, and 4.6 nm, respectively. CdSe@ZnS colloidal NCs were synthesized by means of drop-wise injection of a ZnS precursor stock solution into the mixture. The ZnS shell was grown on the presynthesized CdSe NC core surface. To stop the reaction, the flask was cooled and nonanoic acid was added to avoid the formation of a gel. The prepared NCs were then precipitated by adding a small amount of methanol and repeatedly washed before their redispersion in the selected solvents, namely, $CHCl_3$ and toluene.

Preparation of nanocomposites based on CdSe@ZnS NCs and PS: Fixed amounts of the 1×10^{-5} M CdSe@ZnS NCs in $CHCl_3$ were added to PS in order to prepare nanocomposite solutions with 3 and 5 wt% polymer. The mixtures were gently stirred and then sonicated in a megasonic bath (1 MHz) until the complete dispersion of the $CHCl_3$ solution of NCs in PS and left to rest for a few minutes in order to remove the bubbles formed in solution.

Characterization: The spectroscopic properties of CdSe@ZnS NCs were investigated by UV–Vis absorption and emission spectroscopy using a Varian Cary 5 spectrophotometer and a Varian Eclipse spectrofluorometer, respectively. Relative PL quantum yield of the 2.7-, 3.4-, and 4.7-nm-diameter NC-based solutions were estimated by using fluorescein, rhodamine 101, and rhodamine 6G solutions as reference dyes, respectively, by comparing the integrated fluorescence intensity of the NC solutions with that of the corresponding reference dye, both recorded using excitation solutions of the same absorbance (<0.1 a.u.) in order to minimize possible re-absorption effects.

Optical microscope images of inkjet-printed pixels were recorded with a Nikon Eclipse L200. Fluorescence optical

micrographs were recorded with a Carl Zeiss Axio Vision Product Suite CD25 equipped with an AxioCam MRc 5, where the samples were irradiated with a blue light filter. A Veeco Wyko NT1100 optical profiler was used to observe the surface morphology of the pixels. A Zeiss LEO 1550 SEM was used to observe the pixels and estimate their diameters. Topographic AFM measurements were performed using a PSIA XE-100 SPM System operating in noncontact mode in air using a silicon nitride tip (MLCT-AUHW, Park Scientific) with a cantilever with a spring constant of 0.01 N m^{-1}. Micrographs were collected in height mode by sampling the surface at a scan rate of 0.7 Hz and at a resolution of 512 × 512 pixels. Image were analyzed and processed by using XEI software.

Acknowledgements

J. Y. Kim and C. Ingrosso contributed equally to this work. This work was partially supported by the EC-funded Project NOVOPOLY (Contract no. STRP 013619) and Italian MIUR SINERGY programme (FIRB RBNE03S7XZ).

[1] a) M. Campbell, D. N. Sharp, M. T. Harrison, R. G. Denning, A. J. Turberfield, *Nature* **2000**, *404*, 53; b) B. H. Cumpston, S. P. Ananthavel, S. Barlow, D. L. Dyer, J. E. Ehrlich, L. L. Erskine, A. A. Heikal, S. M. Kuebler, I. Y. S. Lee, D. McCord-Maughon, J. Q. Qin, H. Rockel, M. Rumi, X. L. Wu, S. R. Marder, J. W. Perry, *Nature* **1999**, *398*, 51; c) G. M. Gratson, M. J. Xu, J. A. Lewis, *Nature* **2004**, *428*, 386.

[2] R. D. Piner, J. Zhu, F. Xu, S. H. Hong, C. A. Mirkin, *Science* **1999**, *283*, 661.

[3] B. J. de Gans, P. C. Duineveld, U. S. Schubert, *Adv. Mater.* **2004**, *16*, 203.

[4] H. Sirringhaus, T. Kawase, R. H. Friend, T. Shimoda, M. Inbasekaran, W. Wu, E. P. Woo, *Science* **2000**, *290*, 2123.

[5] H. Ago, K. Murata, M. Yumura, J. Yotani, S. Uemura, *Appl. Phys. Lett.* **2003**, *82*, 811.

[6] Y. Yoshioka, P. D. Calvert, G. E. Jabbour, *Macromol. Rapid Commun.* **2005**, *26*, 238.

[7] V. Marin, E. Holder, M. M. Wienk, E. Tekin, D. Kozodaev, U. S. Schubert, *Macromol. Rapid Commun.* **2005**, *26*, 319.

[8] E. A. Roth, T. Xu, M. Das, C. Gregory, J. J. Hickman, T. Boland, *Biomaterials* **2004**, *25*, 3707.

[9] E. Tekin, E. Holder, V. Marin, B. J. de Gans, U. S. Schubert, *Macromol. Rapid Commun.* **2005**, *26*, 293.

[10] C. B. Murray, C. R. Kagan, M. G. Bawendi, *Annu. Rev. Mater. Sci.* **2000**, *30*, 545.

[11] a) C. Ingrosso, V. Fakhfouri, M. Striccoli, A. Agostiano, A. Voigt, G. Gruetzner, M. L. Curri, J. Brugger, *Adv. Funct. Mater.* **2007**, *17*, 2009; b) M. Tamborra, M. Striccoli, M. L. Curri, J. A. Alducin, D. Mecerreyes, J. A. Pomposo, N. Kehagias, V. Reboud, C. M. Sotomayor Torres, A. Agostiano, *Small* **2007**, *3*, 822.

[12] K. J. Lee, B. H. Jun, T. H. Kim, J. Joung, *Nanotechnology* **2006**, *17*, 2424.

[13] S. H. Ko, H. Pan, C. P. Grigoropoulos, C. K. Luscombe, J. M. J. Frechét, D. Poulikakos, *Nanotechnology* **2007**, *18*, 345202.

[14] E. Tekin, P. J. Smith, S. Hoeppener, A. M. J. van den Berg, A. S. Susha, A. L. Rogach, J. Feldmann, U. S. Schubert, *Adv. Funct. Mater.* **2007**, *17*, 23.

[15] a) T. Leveder, S. Landis, L. Davoust, *Appl. Phys. Lett.* **2008**, *92*, 013107; b) H. Sadabadi, M. Ghasemi, *Polym. Plast. Technol. Eng.* **2008**, *47*, 427.

[16] W. W. Yu, L. H. Qu, W. Z. Guo, X. G. Peng, *Chem. Mater.* **2003**, *15*, 2854.

[17] J. F. Rudd, in *Polymer Handbook*. 3rd ed., (Eds: J. Brandrup, E. H. Immergut), John Wiley & Sons, New York. **1989**, p 81.

[18] a) B. J. de Gans, E. Kazancioglu, W. Meyer, U. S. Schubert, *Macromol. Rapid Commun.* **2004**, *25*, 292; b) B. J. de Gans, L. J. Xue, U. S. Agarwal, U. S. Schubert, *Macromol. Rapid Commun.* **2005**, *26*, 310.

[19] a) T. W. Shield, D. B. Bogy, F. E. Talke, *IBM J. Res. Dev.* **1987**, *31*, 96; b) E. R. Lee, in *Microdrop Generation*, CRC Press, Boca Raton, FL **2003**.

[20] a) F. I. Li, S. M. Thaler, P. H. Leo, J. A. Barnard, *J. Phys. Chem. B* **2006**, *110*, 25838; b) J. Park, J. Moon, *Langmuir* **2006**, *22*, 3506.

[21] a) N. Depalo, R. Comparelli, M. Striccoli, M. L. Curri, P. Fini, L. Giotta, A. Agostiano, *J. Phys. Chem. B* **2006**, *110*, 17388; b) J. E. Bowen Katari, V. L. Colvin, P. Alivisatos, *J. Phys. Chem.* **1994**, *98*, 4109.

Received: September 8, 2008
Revised: November 18, 2008
Published online: